ARTICLE

Stem-Like and Non–Stem Human Pancreatic Cancer Cells Distinguished by Morphology and Metastatic Behavior

Mohamed K. Hassanein,[1,2] Atsushi Suetsugu,[1,2,3] Shigetoyo Saji,[3] Hisataka Moriwaki,[3] Michael Bouvet,[2] A.R. Moossa,[2] and Robert M. Hoffman[1,2]*

[1]AntiCancer, Inc., San Diego, California
[2]Department of Surgery, University of California, San Diego, California
[3]Gifu University Graduate School of Medicine, Gifu, Japan

ABSTRACT

We report here that XPA1 human pancreatic cancer cells are dimorphic. After injection in the spleen, XPA1 cells isolated from the primary tumor in the spleen were predominantly round; while cells isolated from the resulting liver metastasis and ascites were comprised of both round- and spindle-shaped cell types. Cancer cells previously grown in the spleen and re-implanted in the spleen developed large primary tumors in the spleen only. Cancer cells isolated from liver metastasis and re-transplanted to the spleen resulted in a primary tumor in the spleen and liver metastasis. Cancer cells derived from ascites and re-transplanted to the spleen developed primary tumors in the spleen and distant metastasis in the liver, lung, and diaphragm in addition to ascites formation. Spindle and round cells were differentially labeled with fluorescent proteins of different colors. After co-injection of the two cell types in the spleen, cells were isolated from the primary tumors, liver metastasis, and ascites and analyzed by color-coded fluorescence microscopy and fluorescence-activated cell sorting (FACS). No significant differences between the percentages of spindle-shaped and round cancer cells in the primary tumor and the liver metastasis were observed. However, spindle-shaped cancer cells were enriched in the ascites. One hundred percent of the spindle-shaped and round cancer cells expressed CD44, suggesting that morphology and metastatic behavior rather than CD44 expression can distinguish the stem-like cells of the XPA1 pancreatic cancer cell line. The spindle-shaped cancer cells had the greater capability for distant metastasis and ascites formation, suggesting they are stem-like cells, which can be readily targeted for therapy. J. Cell. Biochem. 112: 3549–3554, 2011.
© 2011 Wiley Periodicals, Inc.

INTRODUCTION

Cancers are heterogeneous in cell type and at least some may contain stem-like cells (CSCs) or cancer initiating cells (CICs) which may be similar or identical [Marhaba et al., 2008]. CSCs/CICs are characterized by three major features: (1) potential to differentiate into several or all types of cells that comprise the tumor; (2) self-renewal ability; and (3) capacity to maintain a "stem cell population" [Schulenburg et al., 2010; Kraljevic Pavelic et al., 2011].

Virchow and Paget first referred to the concept of CSCs more than one century ago [Virchow, 1855; Paget, 1889; Lin et al., 2008]. Bonnet and Dick [1997] were the first to isolate CSCs/CICs, from human acute myeloid leukemia. Many studies followed, identifying CSCs/CICs from human solid tumors including colon [Dalerba et al., 2007; Ricci-Vitiani et al., 2007], skin [Prince et al., 2006], brain [Singh et al., 2003], prostate [Collins et al., 2005], and bone [Riggi et al., 2011].

Li et al. [2007] reported that pancreatic cancer cells, with a $CD44^+CD24^+ESA^+$ phenotype, had a 100-fold increased tumorigenic potential. Several other studies have characterized CSCs/CICs in pancreatic cancer [Huang et al., 2008; Ischenko et al., 2010; Yao et al., 2010].

CSCs/CICs may be responsible for important cancer behavior including resistance to chemotherapy and radiotherapy [Lee et al., 2008; Jimeno et al., 2009; Morrison et al., 2011], recurrence after surgical removal and formation of distant metastasis.

Most CSC/CICs have been identified by surface markers such as CD44 in addition to their behavior. In the current study of the XPA1 human pancreatic cancer cell line, we observed that distinct morphology, as well as metastatic behavior, could distinguish CSC-like cells from non-CSC cells.

MATERIALS AND METHODS

CELL LINE AND CULTURE CONDITIONS

The XPA1 human pancreatic cancer cell line expressing red fluorescent protein (RFP) (XPA1-RFP) was used in this study and was a kind gift from Dr. Anirban Maitra. Cells were maintained in RPMI 1640 medium supplemented with 10% fetal bovine serum (FBS) and 2 mM glutamine from Gibco-BRL, Life Technologies Inc. (Grand Island, NY). All media were supplemented with penicillin and streptomycin (Gibco-BRL). Cells were cultured at 37°C with 5% CO_2 [McElroy et al., 2008].

PRODUCTION OF RFP RETROVIRAL VECTOR

The RFP (DsRed-2) gene (Clontech Laboratories, Mountain View, CA) was inserted in the retroviral-based mammalian expression vector pLNCX (Clontech) to form the pLNCX DsRed-2 vector. Production of retrovirus resulted from transfection of pLNCX DsRed-2 in PT67 packaging cells, which produced retroviral supernatants containing the DSRed-2 gene. Briefly, PT67 cells were grown as monolayers in DMEM supplemented with 10% FCS (Gemini Biological Products, Calabasas, CA). Exponentially growing cells (in 10-cm dishes) were transfected with 10 μg expression vector using LipofectAMINE Plus (Life Technologies). Transfected cells were replated 48 h after transfection and 100 μg/ml were added 7 h after transfection. Two days later, the amount of G418 was increased to 200 μg/ml. During the drug selection period, surviving colonies were visualized under fluorescence microscopy and RFP-positive colonies were isolated [Bouvet et al., 2006; Hoffman and Yang, 2006a].

RFP GENE TRANSDUCTION OF XPA1 CELLS

For RFP gene transduction, 20% confluent XPA1 cells were incubated with a 1:1 precipitated mixture of retroviral-containing supernatants of PT67 cells and RPMI 1640 or other culture media (Life Technologies) containing 10% FBS (Gemini Biological Products) for 72 h. Fresh medium was replenished at this time. Cancer cells were harvested with trypsin/EDTA and subcultured at a ratio of 1:15 into selective medium, which contained 50 μg/ml G418. To select brightly fluorescent cells, the level of G418 was increased to 800 μg/ml in a stepwise manner. Clones of cancer cells expressing RFP were isolated with cloning cylinders (Bel-Art Products) by trypsin/EDTA and amplified and transferred by conventional culture methods in the absence of selective agent [Bouvet et al., 2006; Hoffman and Yang, 2006a].

PRODUCTION OF HISTONE H2B–GFP VECTOR

The histone H2B gene has no stop codon, thereby enabling the ligation of the H2B gene to the 5′-coding region of the GFP gene (Clontech Laboratories). The histone H2B-GFP fusion gene was then inserted at the HindIII/CalI site of the pLHCX vector (Clontech Laboratories) that has the hygromycin resistance gene. To establish a packaging cell clone producing high amounts of histone H2B-GFP retroviral vector, the pLHCX histone H2B-GFP plasmid was transfected in PT67 cells using the same methods described above for PT67-DsRed-2. The transfected cells were cultured in the presence of 200–400 μg/ml hygromycin (Life Technologies), increased stepwise to establish stable PT67 H2B-GFP packaging cells [Hoffman and Yang, 2006b].

RFP AND HISTONE H2B–GFP GENE TRANSDUCTION OF CANCER CELLS

To establish dual-color cancer cells, XPA1-RFP cells were incubated with a 1:1 precipitated mixture of retroviral supernatants of PT67 H2B-GFP cells and culture medium. To select the double transformants, the RFP-expressing cancer cells were incubated with hygromycin 72 h after transfection. The level of hygromycin was increased stepwise up to 400 μg/ml and selected in an analogous manner as described above for the RFP cancer cells [Hoffman and Yang, 2006b].

ANIMAL CARE

Nude mice were bred and maintained in a HEPA-filtered environment at the AntiCancer, Inc. vivarium (San Diego, CA) with cages, chow, and bedding sterilized by autoclaving. The animal diets were obtained from Harlan Teklad (Madison, WI). Ampicillin (5.0%, w/v; Sigma, St. Louis, MO) was added to the autoclaved drinking water. All surgical procedures and imaging were performed with the animal anesthetized by intramuscular injection of 0.02 ml of a solution of 50% ketamine, 38% xylazine, and 12% acepromazine maleate. All animal studies were conducted in accordance with the principles of and procedures outlined in the NIH guide for the care and use of laboratory animals under assurance number A3873-1 [Yamauchi et al., 2006].

TRANSPLANTATION OF XPA1 PANCREATIC CANCER CELLS IN THE SPLEEN OF NUDE MICE

In order to inject XPA1 cancer cells in the spleen of nude mice, a laparotomy was performed under anesthesia. XPA1 cancer cells (10^7) were then injected in the spleen using insulin syringes with the BD Ultra-Fine™ needle (BD, Franklin Lakes, NJ), followed by closure of the incision.

FACS ANALYSIS

Fluorescence-activated cell sorting (FACS) was performed using standard protocols. XPA1-RFP cancer cells were labeled with mouse anti-human CD44-FITC antibodies.

ANIMAL IMAGING

The Olympus OV100 Small Animal Imaging System (Olympus Corp., Tokyo, Japan), containing an MT-20 light source (Olympus Biosystems, Planegg, Germany) and DP70 camera (Olympus Corp), was used for mouse imaging [Yamauchi et al., 2006].

IMMUNOCYTOCHEMISTRY

The cancer cells were washed in PBS and then were fixed in 4% paraformaldehyde for 30 min. The wash with PBS was performed then the cells were blocked in PBS with 0.5% BSA for 30 min. Fixed cancer cells were incubated with anti-human FITC-CD44 (BD Pharmingen, Franklin Lakes, NJ) in a moist chamber at 4°C for 12 h. The signal was detected using a fluorescence microscope [Walter et al., 2011].

RESULTS AND DISCUSSION

THE XPA1 HUMAN PANCREATIC CANCER CELL LINE HAS THE CAPABILITY TO FORM DISTANT METASTASIS AND ASCITES

After intrasplenic injection, the XPA1 human pancreatic cancer cell line was able to grow into primary tumors in the spleens of all the five animals injected, resulting in liver metastasis in 4/5 animals and ascites in 3/5 animals (Fig. 1a). The spleens and the livers were dissected and then imaged with the OV100 system to determine the size of the tumors.

XPA1 CELLS ARE DIMORPHIC

XPA1 cancer cells growing in the spleens, livers, and ascites were isolated and observed under fluorescence microscopy. Two different morphological subtypes of XPA1 cells, spindle-shaped and round cells, were observed. Cells isolated from the primary spleen tumor site were comprised mainly of round cells, while the cells from distant metastasis to the liver and ascites comprised a mixture of the two morphological subtypes (Fig. 1b).

CD44 IS EXPRESSED ON BOTH MORPHOLOGICAL XPA1 CELL TYPES

CD44 is a marker expressed by pancreatic CSCs/CICs [Li et al., 2007] as well as other cancers [Ohashi et al., 2007; Lee et al., 2011]. We performed FACS to detect the expression of CD44 in both the primary and the metastatic XPA1 cancer cells. CD44 was expressed in 97.1% of the primary site cancer cells, 98.2% of the liver metastasis cells, and 100% of the cells isolated from the ascites.

TUMORGENICITY AND METASTATIC CAPABILITY OF MORPHOLOGICAL SUBTYPES OF XPA1 CELLS

Three different tumor models were prepared to study tumorgenicity and metastasis of the two morphologic subtypes of XAP1. In the first model, the spleen was injected with 10^7 XPA1 cells isolated from spleen tumors. In the second model, the spleen was injected with 10^7 XPA1 cells isolated from the liver metastases. In the third model, the spleen was injected with 10^7 XPA1 cells isolated from ascites. The mice were followed for 4 weeks and then sacrificed and imaged using the OV100 (Fig. 2). Mice from the first model developed large primary tumors in the spleen in 2/3 mice without any distant
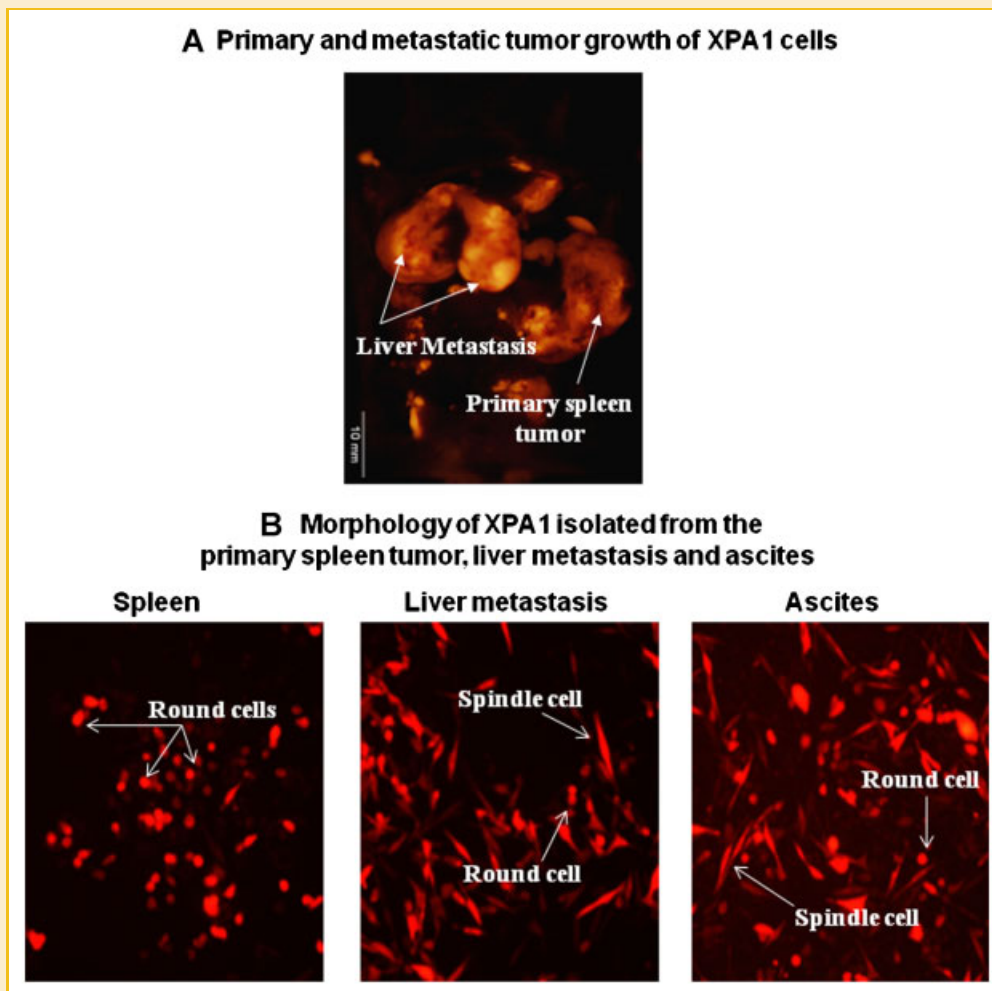

Fig. 1. Primary and metastatic tumor growth of XPA1 cells. A: XPA1 cancer cells grew into primary tumors in the spleen with formation of distant metastasis to the liver. B: Round and spindle morphological subtypes of XPA1 cells. Round cells were predominant in the primary spleen tumor while the liver metastasis and ascites had round and spindle-shaped XPAI cells.

A Cells isolated from primary spleen tumor

B Cells isolated from liver metastasis

C Cells isolated from ascites

D Ability to from lung metastasis from XPA1 cells isolated from various sites
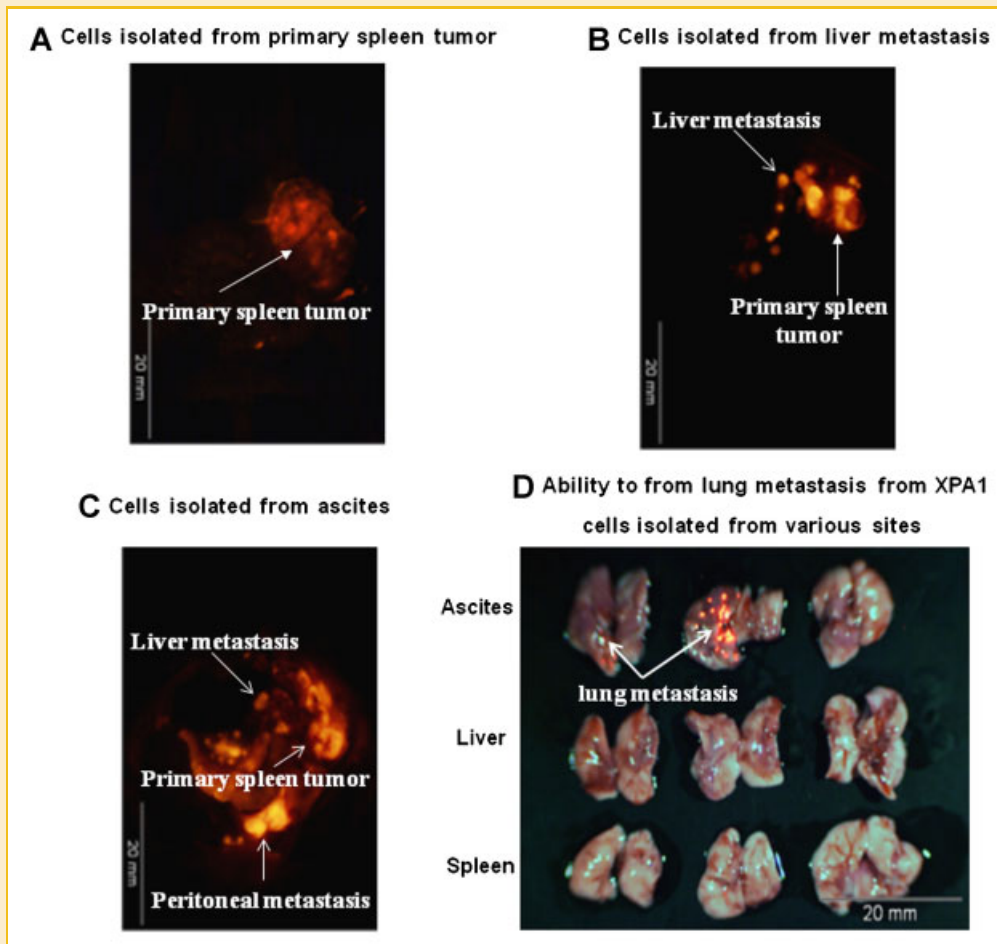
Fig. 2. Growth pattern of XPA1 cells isolated from various sites. Implantation of XPA1 cells isolated from primary spleen tumor, liver metastasis, and ascites. All cells were implanted in the spleen of nude mice. A: Primary tumor growing after implantation of primary spleen tumor cells. B: Primary tumors and metastasis growing after implantation of liver metastasis cells. C: Primary tumors and metastasis growing after implantation of ascites cells. D: Lung metastasis formed only after spleen implantation of ascites cells and not cancer cells from other sites.

metastasis or ascites. The second model developed primary tumor in the spleen in 3/3 mice and distant metastasis to the liver in 1/3 mice. The third model developed primary tumors in the spleen in 3/3 mice, distant metastasis to the liver in 2/3 mice, distant metastasis to the lung in 2/3 mice, distant metastasis to the diaphragm in 3/3 mice and ascites in 3/3 mice. These data demonstrated the enhanced metastasis of the XPA1 cells isolated from ascites.

THE TWO DIFFERENT MORPHOLOGICAL CELL TYPES OF XPA1 HAVE DIFFERENT TUMORIGENIC AND METASTATIC CAPABILITIES

Serial dilution was performed to obtain clones of each cellular morphology for further analysis. A single cancer cell from each morphology formed clones in vitro (Fig. 3). The spindle cells could spread throughout the surface of the culture flask while the round cells tended to grow in a more clumped pattern.

Differences in the tumorigenic and metastatic behavior of the two morphological XPA1 subtypes were determined. The two morphological cellular subtypes were color coded in order to distinguish their behavior. Round cells were labeled with RFP. Spindle cells were double labeled with GFP in their nuclei and RFP in their cytoplasm.

10^7 of each color-coded morphological cellular subtype were co-injected into the spleens of nude mice (n = 12). The animals were followed for 4 weeks and then sacrificed. Tumors were dissected from the spleens and the metastatic organs, including liver, lung, and diaphragm. The organs were imaged with the OV100. Ascites from each animal were also collected. Nine of 12 animals developed primary and metastatic tumors.

There was a direct relationship between the surface area of the sub-diaphragmatic metastasis and the amount of malignant ascites. In contrast, there was not a consistent relationship between the size of the liver metastases and the amount of ascites.

XPA1 cells from the spleens, livers, and ascites were isolated and observed under fluorescence microscopy. The primary tumor from the spleens had more RFP round cells. The malignant ascites was comprised mainly of dual-color spindle cells, while the distant metastasis to the liver was comprised of both RFP round and dual-color spindle cells (Fig. 4).

FACS demonstrated that spindle cells represented 44.6% of the cells in the spleen tumors, 44.8% in the liver metastasis, and 79.1% in the ascites. Round cells represented 47.8% in the spleen, 47.9% in
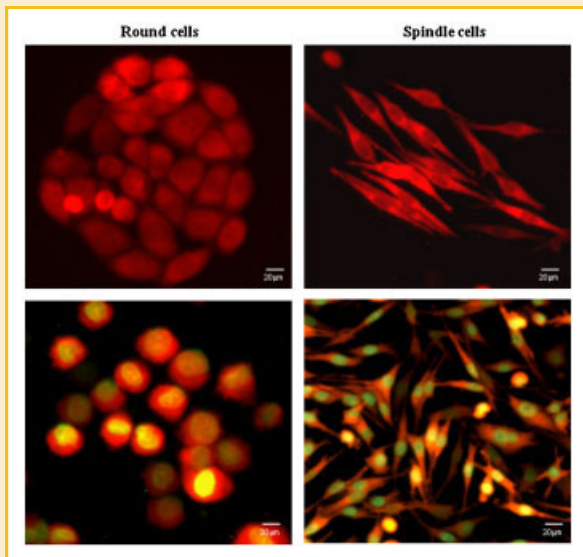
Fig. 3. Cloning of XPA1 round and spindle cancer cells after single cell plating. The upper panel shows RFP cancer cells while the lower panel shows dual-color cancer cells labeled with GFP in the nucleus and RFP in the cytoplasm.

the liver, and 17.3% in the ascites. These data revealed that both cell types have a similar capacity to grow in the primary injection site. Both spindle and round cells also have a similar capability to form liver metastasis. However, spindle cells comprised the large majority of ascites (Fig. 4b).

Kabashima et al. [2009] showed that a side population of pancreatic cancer cells, enriched in CSCs, changed their shape into a mesenchymal-like appearance, including spindle-shaped cells. The spindle-shaped cells had less cell adhesion proteins, a characteristic which enabled the cells to be more mobile and able to migrate to distant sites. In the present study, the presence of spindle cells in a high percentage in the ascites suggests two important characteristics of these cells: (A) the mesenchymal like morphology of these cells may have enabled them to escape from the tumor vasculature to the peritoneal cavity, (B) these cells can grow without anchorage, a characteristic of highly malignant cells [Berezovska et al., 2006].

CD44 was expressed in 100% of spindle and round cells in all spleen, liver, and ascites cells. Thus, CD44 does not distinguish the morphologic cellular subtypes and cannot identify XPA1 CSCs.

In the co-implantation experiments, no significant differences between the percentages of spindle-shaped and round cancer cells in the primary tumor and the liver metastasis were observed. However, spindle-shaped cancer cells were enriched in the ascites. The data
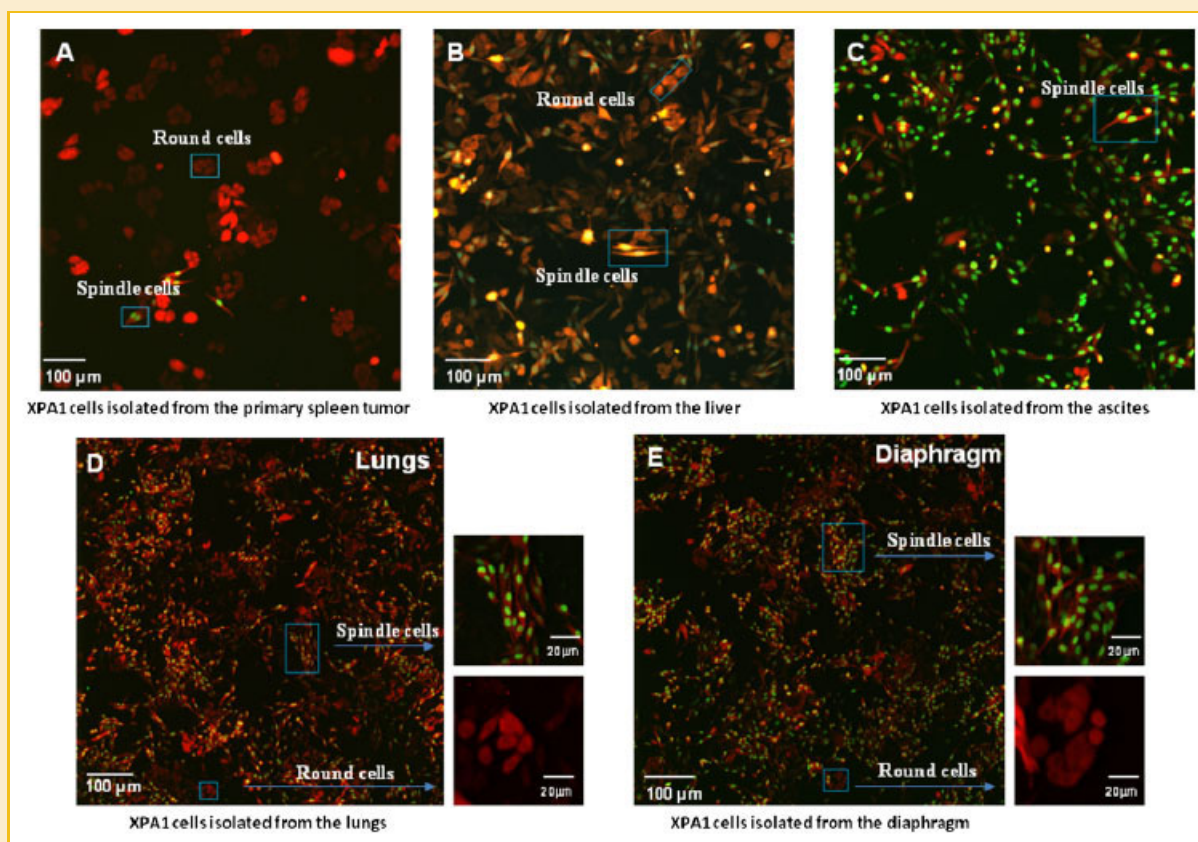

Fig. 4. In vitro culture of the XPA1 cells isolated from different sites. Distribution of XPA1 spindle and round cells in (A) primary spleen tumor, (B) liver metastasis, (C) ascites, (D) lungs, and (E) diaphragm.

presented here suggest that morphology and metastatic behavior, rather than CD44, can identify the stem-like cells of the XPA1 pancreatic cancer cell line. The spindle-shaped cancer cells had the greater capability for distant metastasis and ascites formation, suggesting they may be CSCs, which can be readily targeted.

REFERENCES

Berezovska OP, Glinskii AB, Yang Z, Li XM, Hoffman RM, Glinsky GV. 2006. Essential role for activation of the Polycomb Group (PcG) protein chromatin silencing pathway in metastatic prostate cancer. Cell Cycle 5:1886–1901.

Bonnet D, Dick JE. 1997. Human acute myeloid leukemia is organized as a hierarchy that originates from a primitive hematopoietic cell. Nat Med 3(7):730–737.

Bouvet M, Tsuji K, Yang M, Jiang P, Moossa AR, Hoffman RM. 2006. In vivo color-coded imaging of the interaction of colon cancer cells and splenocytes in the formation of liver metastases. Cancer Res 66(23):11293–11297.

Collins AT, Berry PA, Hyde C, Stower MJ, Maitland NJ. 2005. Prospective identification of tumorigenic prostate cancer stem cells. Cancer Res 65(23):10946–10951.

Dalerba P, Dylla SJ, Park IK, Liu R, Wang X, Cho RW, Hoey T, Gurney A, Huang EH, Simeone DM, Shelton AA, Parmiani G, Castelli C, Clarke MF. 2007. Phenotypic characterization of human colorectal cancer stem cells. Proc Natl Acad Sci USA 104(24):10158–10163.

Hoffman RM, Yang M. 2006a. Color-coded fluorescence imaging of tumor-host interactions. Nat Protoc 1:928–935.

Hoffman RM, Yang M. 2006b. Subcellular imaging in the live mouse. Nat Protoc 1:775–782.

Huang P, Wang CY, Gou SM, Wu HS, Liu T, Xiong JX. 2008. Isolation and biological analysis of tumor stem cells from pancreatic adenocarcinoma. World J Gastroenterol 14(24):3903–3907.

Ischenko I, Seeliger H, Kleespies A, Angele MK, Eichhorn ME, Jauch KW, Bruns CJ. 2010. Pancreatic cancer stem cells: New understanding of tumorigenesis, clinical implications. Langenbecks Arch Surg 395:1–10.

Jimeno A, Feldmann G, Suárez-Gauthier A, Rasheed Z, Solomon A, Zou GM, Rubio-Viqueira B, García-García E, López-Ríos F, Matsui W, Maitra A, Hidalgo M. 2009. A direct pancreatic cancer xenograft model as a platform for cancer stem cell therapeutic development. Mol Cancer Ther 8(2):310–314.

Kabashima A, Higuchi H, Takaishi H, Matsuzaki Y, Suzuki S, Izumiya M, Iizuka H, Sakai G, Hozawa S, Azuma T, Hibi T. 2009. Side population of pancreatic cancer cells predominates in TGF-β-mediated epithelial to mesenchymal transition and invasion. Int J Cancer 124:2771–2779.

Kraljevic Pavelic S, Sedic M, Bosnjak H, Spaventi S, Pavelic K. 2011. Metastasis: New perspectives on an old problem. Mol Cancer 10:22.

Lee HE, Kim JH, Kim YJ, Choi SY, Kim SW, Kang E, Chung IY, Kim IA, Kim EJ, Choi Y, Ryu HS, Park SY. 2011. An increase in cancer stem cell population after primary systematic therapy is a poor prognostic factor in breast cancer. Br J Cancer 104(11):1730–1738.

Lee CJ, Li C, Simeone DM. 2008. Human pancreatic cancer stem cells: Implications for how we treat pancreatic cancer. Transl Oncol 1(1):14–18.

Li C, Heidt DG, Dalerba P, Burant CF, Zhang L, Adsay V, Wicha M, Clarke MF, Simeone DM. 2007. Identification of pancreatic cancer stem cells. Cancer Res 67(3):1030–1037.

Lin EH, Jiang Y, Deng Y, Lapsiwala R, Lin T, Blau CA. 2008. Cancer stem cells, endothelial progenitors, and mesenchymal stem cells: "Seed and Soil" theory revisited. Gastrointestinal Cancer Res 2(4):169–174.

Marhaba R, Klingbeil P, Nuebel T, Nazarenko I, Buechler MW, Zoeller M. 2008. CD44 and EpCAM: Cancer-initiating cell markers. Curr Mol Med 8(8):784–804.

McElroy M, Kaushal S, Bouvet M, Hoffman RM. 2008. Color-coded imaging of splenocyte-pancreatic cancer cell interactions in the tumor microenvironment. Cell Cycle 7(18):2916–2921.

Morrison R, Schleicher SM, Sun Y, Niermann KJ, Kim S, Spratt DE, Chung CH, Lu B. 2011. Targeting the mechanisms of resistance to chemotherapy and radiotherapy with the cancer stem cell hypothesis. J Oncol 941876.

Ohashi R, Takahashi F, Cui R, Yoshioka M, Gu T, Sasaki S, Tominaga S, Nishio K, Tanabe KK, Takahashi K. 2007. Interaction between CD44 and hyaluronate induces chemoresistance in non-small cell lung cancer cell. Cancer Lett 252(2):225–234.

Paget S. 1889. The distribution of secondary growths in cancer of the breast. Lancet 1:571–573.

Prince ME, Sivanandan R, Kaczorowski A, Wolf GT, Kaplan MJ, Dalerba P, Weissman IL, Clarke MF, Ailles LE. 2006. Identification of a subpopulation of cells with cancer stem cell properties in head and neck squamous cell carcinoma. Proc Natl Acad Sci USA 104(3):973–978.

Ricci-Vitiani L, Lombardi DG, Pilozzi E, Biffoni M, Todaro M, Peschle C, De Maria R. 2007. Identification and expansion of human colon-cancer-initiating cells. Nature 445:111–115.

Riggi N, Suvà ML, Stamenkovic I. 2011. The cancer stem cell paradigm in Ewing's sarcoma: What can we learn about these rare cells from a rare tumor? Expert Rev Anticancer Ther 11(2):143–145.

Schulenburg A, Brämswig K, Herrmann H, Karlic H, Mirkina I, Hubmann R, Laffer S, Marian B, Shehata M, Krepler C, Pehamberger H, Grunt T, Jäger U, Zielinski CC, Valent P. 2010. Neoplastic stem cells: Current concepts and clinical perspectives. Crit Rev Onc Hemat 76:79–98.

Singh SK, Clarke ID, Terasaki M, Bonn VE, Hawkins C, Squire J, Dirks PB. 2003. Identification of a cancer stem cell in human brain tumors. Cancer Res 63:5821–5828.

Virchow R. Editorial. 1855. Virchows Arch Pathol Anat Physiol Klin Med 3.

Walter D, Satheesha S, Albrecht P, Bornhauser BC, D'Alessandro V, Oesch SM, Rehrauer H, Leuschner I, Koscielniak E, Gengler C, Moch H, Bernasconi M, Niggli FK, Schäfer BW; CWS Study Group. 2011. CD133 positive embryonal rhabdomyosarcoma stem-like cell population is enriched in rhabdospheres. PLoS One 6(5):e19506.

Yamauchi K, Yang M, Jiang P, Xu M, Yamamoto N, Tsuchiya H, Tomita K, Moossa AR, Bouvet M, Hoffman RM. 2006. Development of real-time subcellular dynamic multicolor imaging of cancer-cell trafficking in live mice with a variable-magnification whole-mouse imaging system. Cancer Res 66:4208–4214.

Yao J, Cai HH, Wei JS, An Y, Ji ZL, Lu ZP, Wu JL, Chen P, Jiang KR, Dai CC, Qian ZY, Xu ZK, Miao Y. 2010. Side population in the pancreatic cancer cell lines SW1990 and CFPAC-1 is enriched with cancer stem-like cells. Oncol Rep 23:1375–1382.